

Fourier integral operators, phase-screens, and their relationship to statics correction: An example from offshore Norway

Robert J. Ferguson, University of Texas, Austin; Charles M. Mosher, ChevronTexaco

SUMMARY

The Donna Terrace West prospect is located offshore of Nordland, Norway. Hydrocarbon-bearing sands are found in the Cretaceous and Jurassic zones between 2 seconds and 5 seconds on time processed seismic data. A secondary target lies between 1 second and 2 seconds in the Tertiary. Data in this area show poor reflectivity with a low signal to noise ratio in the lower Tertiary and Cretaceous zones. Time-based processing and imaging are used to determine the structure and fluid content of sands in this area. This strategy is most successful when lateral velocity-variation is smooth. At the seafloor is an overburden of glacial till whose topography varies by hundreds of meters across the prospect. The resulting lateral contrast in velocity distorts subsequent layers on time-based sections. As a remedy, datuming is used to remove the effect of the till layer. Beginning with a general expression for one-way operators, a datuming procedure is derived. Motivated by the high cost of the general operator procedure, fast datuming by phase-screen is derived. Both the general procedure and the phase-screen methods are compared to statics correction. Datuming using a screen-operator provides a good balance between the accurate but expensive general operator and the highly approximate statics method. The phase-screen method is used to datum two seismic lines from Donna Terrace West. Comparison with the undatumed data shows significant improvement.

INTRODUCTION

The Donna Terrace West prospect is located offshore of Nordland, Norway (Figure 1). Seismic data in this area show poor reflectivity with a low signal to noise ratio in the lower Tertiary and Cretaceous zones. Hydrocarbon-bearing sands are found in the Cretaceous and Jurassic zones between 2s and 5s on time-processed seismic-data. A secondary target lies between 1s and 2s in the Tertiary.

The top of the geologic column is a layer of glacial till (Figure 2). Its surface is highly reflective and causes strong multiple reflections. Also, this surface is rugose and causes a loss of continuity in underlying reflections. Velocity in the till layer is roughly constant at 2100m/s.

Time processing and imaging can be useful in determining the structure and fluid content of subsurface media, and is most successful if lateral velocity-variation is smooth. In areas of strong variation, time processing may be inadequate, and depth processing and imaging must be contemplated. At Donna Terrace West, strong velocity-contrasts are thought to be confined to the till layer, with fairly constant lateral-velocity in the media below. Time processing is preferred to depth processing because of cost, and the deleterious effects of the till layer are accounted for after processing by shifting the stacked traces.

Instead, by placing a component of depth imaging before time processing, wave-equation datuming (Berryhill, 1985) can be used to mitigate the effects of strongly variable surface-layers like the till layer in Donna Terrace West without increasing cost dramatically. A model of the water column and overburden is built, and the amplitude and phase effects of propagation from the source to the base of the model and up to the recording surface are simulated. Then the amplitude and phase effects are removed from the recorded data. A replacement velocity is then used to correct the recorded data to a regional datum.

Here, we develop and implement a wave-equation datuming method based on recursive explicit extrapolators. These extrapolators accommodate strong variation in velocity, don't require raytracing and are expected to preserve amplitude fidelity.

Two seismic lines are processed through migration to a final stacked-

image, with and without datuming for comparison. The datumed final-section shows superior reflection continuity.

Removal of the effects of the overburden by datuming

In time migration, smooth variation in velocity in the lateral direction is assumed. Departures from smoothness cause reflection events to be distorted and the more expensive process of depth migration may be required. In sedimentary basins where reflectors often lie fairly parallel, the large scale variation in seismic velocity is generally smooth and time migration results in an accurate image for low cost. Frequently, though, some aspect of the near surface causes strong lateral variation that interferes with good imaging of what might otherwise be a simple imaging problem.

On land, a recording surface that follows the surface topography may undulate strongly and distort reflections by adding differential travel-times between sources and receivers. Similarly overburden that is unconsolidated and of variable saturation can exhibit enough variation in velocity to exceed the smoothness requirement and cause further distortion. As a remedy, a model of the overburden can be constructed, and a datum chosen to correspond to the lowest elevation. Traces are then corrected by adding or subtracting travel times between the recording surface and the datum. Vertical propagation of the source and recorded wavefields is assumed in this process. Often, a reference velocity is used to correct from the datum local to the survey, to a datum local to the prospect.

Due to the ability of modern recording systems to control the depth of the streamer, data from marine environments is recorded at a flat recording surface. Also, the uppermost layers are either incompressible and saturated (the water column) or unconsolidated and saturated (the seafloor layer) and are generally assumed to be homogeneous. Datuming is usually not required, and time migration can proceed with accuracy.

In regions like Donna Terrace West, however, the sea floor is composed of unconsolidated glacial till that has significant topographical relief (Figure 2). This rapid variation in elevation imparts a significant lateral contrast in velocity, not because the till layer itself varies in velocity (as will be demonstrated), but simply because of the lateral contrast between the constant till velocity and the constant water velocity.

Datuming using the wave equation

The most general way to datum seismic data is using a procedure based strictly on the wave equation. This can be prohibitively expensive, especially in 3D, and is prone to error when the velocity of the upper layers is not strictly known. Alternative methods that are fast and robust are often based on Kirchoff migration (Wiggins, 1984), or using one-way extrapolation operators (Berryhill, 1984).

The one-way extrapolation operators have the advantage over the Kirchoff methods in that they tolerate strong lateral gradients, as is the case with the water/till interface in Donna Terrace West, though usually at the expense of preservation of high dips. In Donna Terrace West, dip on the reflectors of interest is thought to be gentle ($< 45^\circ$), so the one-way operator may be preferred. Examples of explicit operators are Fourier finite difference (Claerbout and Doherty, 1972), phase shift plus interpolation (Gazdag and Sguazzero, 1984), Generalized phase screen (Le Rousseau and de Hoop, 2001), (Wu and Huang, 1992) and Split step Fourier (Stoffa et al., 1990).

A general expression for one-way wavefield extrapolation through distance z can be written as a Fourier integral operator (Margrave and

Ferguson, 1999; Le Rousseau and de Hoop, 2001):

$$\Psi_R(\mathbf{x}, z) = \int \Psi_R(\mathbf{x}_0, 0) W(\mathbf{x}_0, \mathbf{x}, z) d\mathbf{x}_0, \quad (1)$$

where monochromatic wavefield $\Psi_R(\mathbf{x}_0, 0, \omega)$ (temporal frequency ω is explicitly given) is

$$\Psi_R(\mathbf{x}_0, 0, \omega) = \frac{1}{2\pi} \int \tilde{\Psi}_R(\mathbf{x}_0, 0, t) e^{-i\omega t} dt. \quad (2)$$

Wavefield $\tilde{\Psi}_R$ is a wavefield recorded at depth $z = 0$ with spatial coordinates \mathbf{x}_0 . Extrapolation operator W is given by

$$W(\mathbf{x}_0, \mathbf{x}, z) = \frac{1}{(2\pi)^2} \int e^{izk_z(\mathbf{x}, \mathbf{k})} e^{-\mathbf{k} \cdot [\mathbf{x} - \mathbf{x}_0]} d\mathbf{k}. \quad (3)$$

Vertical wavenumber k_z is related to horizontal wavenumber \mathbf{k} , velocity v , and frequency ω by

$$k_z(\mathbf{x}, \mathbf{k}, \omega) = \sqrt{\left(\frac{\omega}{v(\mathbf{x}; \mathbf{k}, \omega)}\right)^2 - \mathbf{k} \cdot \mathbf{k}}, \quad (4)$$

where ω has been written explicitly. Spatial variation of v is indicated by its dependence on \mathbf{x} . Variation with direction (anisotropy) is indicated by its dependence on \mathbf{k} and ω . Variation in z is constant, and equation (1) represents propagation through a laterally variable medium.

For a medium that varies between $z = 0$ and $z = z_d$ (z_d is a datum), v can be divided into constant velocity layers such that

$$v(\mathbf{x}_d, z_d; \mathbf{k}, \omega) \approx \begin{bmatrix} v(\mathbf{x}_0, \Delta z_0; \mathbf{k}, \omega) \\ v(\mathbf{x}_1, \Delta z_1; \mathbf{k}, \omega) \\ \vdots \\ v(\mathbf{x}_d, \Delta z_d; \mathbf{k}, \omega) \end{bmatrix}, \quad (5)$$

where Δz_j is small, and

$$z_d = \sum_{j=1}^d \Delta z_j. \quad (6)$$

Extrapolation of $\Psi_R(z = 0)$ to datum z_d can then be computed recursively using equation (1)

$$\Psi_R(\mathbf{x}_d, z_d) = \int \Psi_R(\mathbf{x}_0, 0) W(\mathbf{x}_0, \mathbf{x}_d, z_d) d\mathbf{x}_0 \quad (7)$$

where the effective operator W is

$$\begin{aligned} W(\mathbf{x}_0, \mathbf{x}_d, z_d) &= \int W(\mathbf{x}_0, \mathbf{x}_1, \Delta z_1) W(\mathbf{x}_1, \mathbf{x}_2, \Delta z_2) \cdots W(\mathbf{x}_{d-1}, \mathbf{x}_d, \Delta z_d) \\ &\quad d\mathbf{x}_1 d\mathbf{x}_2 \cdots d\mathbf{x}_{d-1} \\ &= \int \prod_{j=1}^d W(\mathbf{x}_{j-1}, \mathbf{x}_j, \Delta z_j) \prod_{j=1}^{d-1} d\mathbf{x}_j. \end{aligned} \quad (8)$$

For the receivers in a common shot gather, equation (8) removes the amplitude and angle dependent effects due to propagation of the reflected wavefield through the overburden.

For a model of the source, recursive extrapolation of the source wavefield Ψ_S :

$$\Psi_S(\mathbf{x}_d, z_d) = \int \Psi_S(\mathbf{x}_0, 0) W(\mathbf{x}_0, \mathbf{x}_d, -z_d) d\mathbf{x}_0. \quad (9)$$

approximates amplitude and angle dependent effects due to propagation from $z = 0$ to z_d . In equation (9), the $(-)$ sign on z_d indicates forward propagation.

The amplitude and phase terms of the source wavefield $\Psi_S(z_d)$ contain all of the information needed to correct $\Psi_R(z_d)$ for propagation of the source through the overburden to z_d . To apply the source correction, form the quotient

$$\tilde{\Psi}_R(\mathbf{x}_n, z_d) = \frac{\Psi_R(\mathbf{x}_n, z_d)}{\Psi_S(\mathbf{x}_n, z_d)} = \frac{\mathcal{A}_R(\mathbf{x}_n, z_d)}{\mathcal{A}_S(\mathbf{x}_n, z_d)} e^{i[\phi_R(\mathbf{x}_n, z_d) - \phi_S(\mathbf{x}_n, z_d)]}, \quad (10)$$

where \mathcal{A}_R and \mathcal{A}_S are the amplitudes of the receiver and source, and ϕ_R and ϕ_S are the phases.

If processing from a regional datum z_d is desired, a second set of amplitude and phases are applied. These amplitudes and phases correspond to propagation from source location on the regional datum z_r down to local datum z_d , and up from there to the receivers on the regional datum z_r ; all at a replacement velocity v_r . Correction to the regional datum z_r is given by:

$$\tilde{\Psi}_R(\mathbf{x}_r, z_r) = \int \tilde{\Psi}_R(\mathbf{x}_d, z_d) \tilde{\Psi}_S(\mathbf{x}_d, z_d) X(\mathbf{x}_r, \mathbf{x}_d, z_d) d\mathbf{x}_d, \quad (11)$$

where

$$X(\mathbf{x}_r, \mathbf{x}_d, z_d) = \frac{1}{(2\pi)^2} \int e^{-iz_d k_z(\mathbf{k})} e^{-i\mathbf{k} \cdot [\mathbf{x}_r - \mathbf{x}_d]} d\mathbf{k}, \quad (12)$$

and

$$k_z(\mathbf{k}, \omega) = \sqrt{\left(\frac{\omega}{\bar{v}}\right)^2 - \mathbf{k} \cdot \mathbf{k}}. \quad (13)$$

Replacement velocity \bar{v} is a regional value chosen such that, on average, reflections are returned close to their original intercept times. The source term $\tilde{\Psi}_S$ in equation (11) is:

$$\tilde{\Psi}_S(\mathbf{x}_n, z_d) = \int \tilde{\Psi}_S(\mathbf{x}_0, 0) X(\mathbf{x}_0, \mathbf{x}_n, z_d) d\mathbf{x}_0. \quad (14)$$

The computational cost of correction to the regional datum using equation (11) is proportional to the cost of the fast Fourier transform $MN \log_2(MN)$, where M and N are, respectively, the inline and crossline dimensions of the recording aperture. This cost is equivalent to the cost of applying, for example, a fan filter in the Fourier domain.

Correction to the local datum using equation (10), however, requires a more substantial computation that is proportional to $MN[M+N]$. This cost is equivalent to applying n fan filters in the Fourier domain without the benefit of the fast Fourier transform. Given the high cost, particularly the cost of datuming to the local datum, it is desirable to have inexpensive alternatives.

Phase screen datuming

Reducing the cost of datuming is possible by approximating the W operators given above. For this paper, we select the phase-screen operator based method as a depth migration code based on this operator was available for conversion into a datuming algorithm.

As demonstrated in Le Rousseau and de Hoop (Le Rousseau and de Hoop, 2001), wavefield extrapolation using equation (1) can be approximated using a truncated series expansion of the k_z term (equation 4)

$$k_z(\mathbf{x}_j, \mathbf{k}, \Delta z_j) \approx \hat{k}_z(\mathbf{x}_j, \Delta z_j) + \bar{k}_z(\mathbf{k}, \Delta z_j) \quad (15)$$

where

$$\hat{k}_z(\mathbf{x}_j, \omega, \Delta z_j) = \frac{v_a(\Delta z_j)}{2\omega} \left[\left(\frac{\omega}{v(\mathbf{x}_j, \Delta z_j)} \right)^2 - \left(\frac{\omega}{v_a(\Delta z_j)} \right)^2 \right], \quad (16)$$

$$\bar{k}_z(\mathbf{k}, \omega, \Delta z_j) = \sqrt{\left(\frac{\omega}{v_a(\Delta z_j)}\right)^2 - \mathbf{k} \cdot \mathbf{k}}, \quad (17)$$

and v_a is a reference velocity for depth Δz_j . Reference velocity v_a is usually chosen to minimize dip filtering, and leakage from the evanescent region. Equation (15) is the simplest and least costly of a class of fast, approximate operators (Le Rousseau and de Hoop, 2001).

Using equation (15), datuming using equation (7) becomes

$$\Psi_R(\mathbf{x}_d, z_d) \approx \int \Psi_R(\mathbf{x}_0, 0) W_{PS}(\mathbf{x}_0, \mathbf{x}_d, z_d) d\mathbf{x}_0, \quad (18)$$

with effective operator

$$W_{PS}(\mathbf{x}_0, \mathbf{x}_d, z_d) = \int e^{i\sum_{j=1}^d \Delta z_j \bar{k}_z(\mathbf{x}_j, \Delta z_j)} \prod_{j=1}^d \bar{W}(\mathbf{x}_{j-1}, \mathbf{x}_j, \Delta z_j) \prod_{j=1}^{d-1} d\mathbf{x}_j, \quad (19)$$

where

$$\bar{W}(\mathbf{x}_{j-1}, \mathbf{x}_j, \Delta z_j) = \frac{1}{(2\pi)^2} \int e^{i\Delta z_j \bar{k}_z(\mathbf{k}, \Delta z_j)} e^{-i\mathbf{k} \cdot (\mathbf{x}_j - \mathbf{x}_{j-1})} d\mathbf{k}. \quad (20)$$

The use of equation (15) instead of equation (1) replaces the slow Fourier transform in the general expression with a fast Fourier transform. The result is a significant reduction in cost.

Datuming by statics correction

The most familiar form of datuming, statics correction, finds application in many onshore exploration prospects. The statics correction method can be derived directly from the general datuming method described by equation (10). We must assume, however, that propagation down from the source through the overburden is vertical, and propagation of the reflected wavefield up into the receivers is also vertical. We may then expand k_z (equation 4) about $\mathbf{k} \cdot \mathbf{k} = 0$ to get

$$k_z(\mathbf{x}_j, \mathbf{k}, \omega, \Delta z_j) \approx k_z(\mathbf{x}_j, \omega, \Delta z_j) = \frac{\omega}{v(\mathbf{x}_j, \Delta z_j)}, \quad (21)$$

and the datumed wavefield $\hat{\Psi}_R(\mathbf{x}_0, 0)$ is computed:

$$\hat{\Psi}_R(\mathbf{x}_0, 0) = \Psi_R(\mathbf{x}_0, 0) e^{i\omega \left\{ \sum_{j=1}^d \Delta z_j \left[\frac{1}{v(\mathbf{x}_j, \Delta z_j)} + \frac{1}{v(\mathbf{x}_S, \Delta z_j)} \right] - 2d \frac{\omega}{v} \right\}} \quad (22)$$

The use of equation (21) in place of equation (4) greatly simplifies the computational aspects of datuming by removing the spatial Fourier transforms from the calculations.

Cost vs. accuracy

The computational cost of each method can be compared relative to the cost of applying a fan filter in Fourier space. For n layers in the velocity model, the general method (equation 1) has a cost equivalent to applying n fan filters using the slow Fourier transform. The cost of using the screen operator (equation 18) is similar to that of the general operator but with the benefit of the fast Fourier transform. Compared to the two previous methods, statics corrections are essentially free of charge.

Analysis of the impulse responses of datuming in rugose media reveals differences between the slow Fourier integral method, the fast phase-screen method, and the ultra-fast statics method. Differences are related to the rugosity of the seafloor, and the contrast between water velocity and seafloor velocity. For Donna Terrace West, the authors find that the phase screen method returned the best compromise between accuracy and efficiency.

WAVE-EQUATION DATUMING OF A 2D LINE

The required depth-to-seafloor is obtained using NMO/DMO and Stolt

migration (parameterized with water velocity) of the near traces. Analysis of first breaks reveals a till velocity of 2100 m/s. Shallow depth-migration of the near offset traces verifies the lateral homogeneity of the till velocity.

In Figures (3) and (4), time-migrated sections are given. The images are the result of identical processing and time migration with datuming Figure (4) being the only difference. The image without datuming Figure (3) shows the pattern of the top of the till layer superimposed on all subsequent structures, with significant pull up below the topographic high at 30 km distance. The image with datuming Figure (4) shows much simpler structure on all features below the till layer, with an absence of pull up beneath the topographic high.

Figures (5) and (6) are similarly processed sections from a tying line. Again, datuming provides significant improvement in image quality.

CONCLUSIONS

A layer of glacial till lying at the seafloor of the Donna Terrace West prospect causes distortion of reflections when time migration is used. Distortion is due mainly to the strong lateral-contrast resulting from the rugosity of the surface of the till layer. To allow interpreters to continue to enjoy the low cost of time processing, wave-equation datuming is employed to remove the effect of the till layer. Datuming by extrapolation is favored over static correction for its superior handling of amplitudes and dipping events. Data examples from Norway show improved imaging of reflection events.

ACKNOWLEDGMENTS

The authors gratefully acknowledge Fugro Multi Client Services for permission to publish the non-exclusive seismic data contained in this paper.

REFERENCES

- Berryhill, J. R., 1984, Wave equation datuming before stack (short note): *Geophysics*, **49**, no. 11, 2064–2067.
- Berryhill, J. R., 1985, Wave equation datuming *in* Gardner, G. H. F., Ed., *Migration of seismic data*: Soc. Expl. Geophys., 331–346.
- Claerbout, J. F., and Doherty, S. M., 1972, Downward continuation of moveout-corrected seismograms: *Geophysics*, **37**, no. 05, 741–768.
- Gazdag, J., and Sguazzero, P., 1984, Migration of seismic data by phase-shift plus interpolation: *Geophysics*, **49**, no. 02, 124–131.
- Le Rousseau, J. H., and de Hoop, M. V., 2001, Modeling and imaging with the scalar generalized-screen algorithms in isotropic media: *Geophysics*, **66**, 1551–1568.
- Margrave, G. F., and Ferguson, R. J., 1999, Wavefield extrapolation by nonstationary phase shift: *Geophysics*, **64**, no. 04, 1067–1078.
- Stoffa, P. L., Fokkema, J. T., de Luna Freire, R. M., and Kessinger, W. P., 1990, Split-step Fourier migration: *Geophysics*, **55**, no. 04, 410–421.
- Wiggins, J. W., 1984, Kirchhoff integral extrapolation and migration of nonplanar data: *Geophysics*, **49**, no. 08, 1239–1248.
- Wu, R.-S., and Huang, L.-J., 1992, Scattered field calculation in heterogeneous media using phase-screen propagation: 62nd Annual Internat. Mtg., Soc. Expl. Geophys., Expanded Abstracts, 1289–1292.



Figure 1: Map of Scandinavia. Donna Terrace West is within the mid-Norway outline.

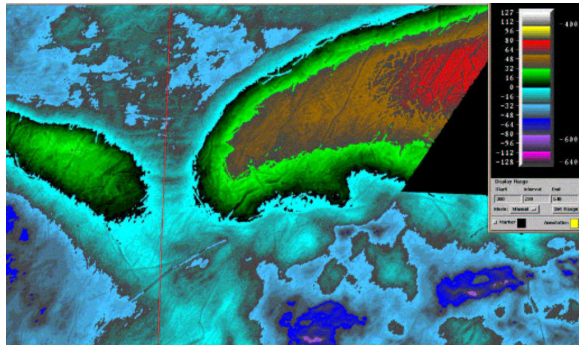


Figure 2: Surface of the glacial till. The map is 50×100 km. High elevations are red, brown and green. Low elevations are light blue through dark blue. Topographic variation is 100's of meters in some areas.

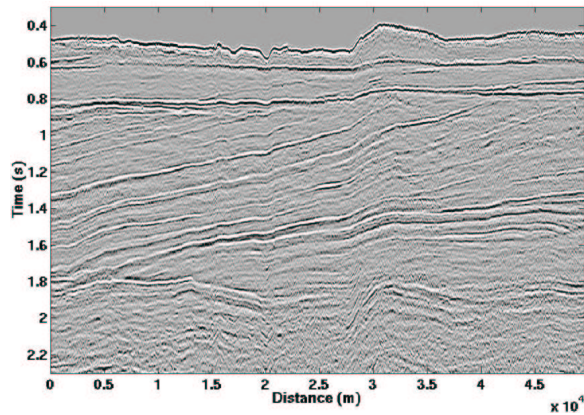


Figure 3: Final image from time processing. The topography of the surface of the till is present on all reflectors.

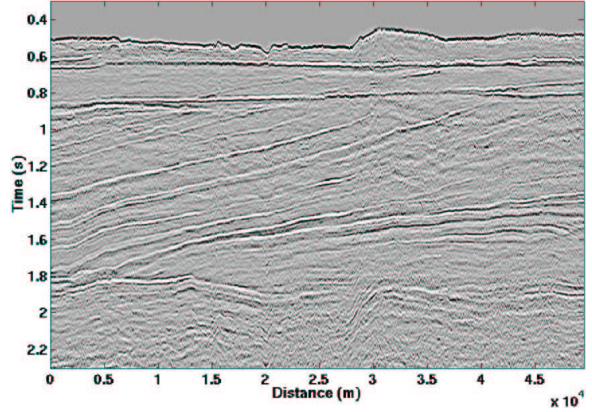


Figure 4: Final image with datuming followed by time processing. Reflectors are flatter after datuming.

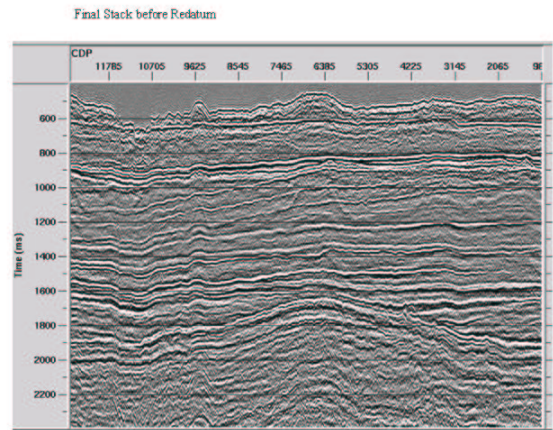


Figure 5: Final image from time processing. The topography of the surface of the till is present on all reflectors.

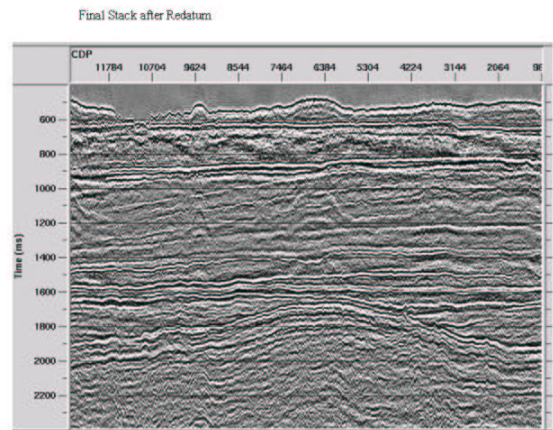


Figure 6: Final image with datuming followed by time processing. Reflectors are flatter after redatuming.